



OPEN ACCESS

EDITED BY

Praveen Sathiyamoorthi,
Indian Institute of Technology (BHU),
India

REVIEWED BY

Nicanor Cimpoesu,
Gheorghe Asachi Technical University
of Iași, Romania
Peilei Zhang,
Shanghai University of Engineering
Sciences, China

*CORRESPONDENCE

Ali Oguz Er,
✉ ali.er@wku.edu

SPECIALTY SECTION

This article was submitted to
Mechanical Properties of Metals,
a section of the journal
Frontiers in Metals and Alloys

RECEIVED 04 November 2022

ACCEPTED 06 December 2022

PUBLISHED 05 January 2023

CITATION

Khuzhakulov Z, Kylychbekov S,
Allamyradov Y, Majidov I, Ben Yosef J,
Er AY, Kitchens C, Banga S,
Badarudeen S and Er AO (2023),
Formation of picosecond laser-induced
periodic surface structures on steel for
knee arthroplasty prosthetics.
Front. Met. Alloy 1:1090104.
doi: 10.3389/ftmal.2022.1090104

COPYRIGHT

© 2023 Khuzhakulov, Kylychbekov,
Allamyradov, Majidov, Ben Yosef, Er,
Kitchens, Banga, Badarudeen and Er.
This is an open-access article
distributed under the terms of the
Creative Commons Attribution License
(CC BY). The use, distribution or
reproduction in other forums is
permitted, provided the original
author(s) and the copyright owner(s) are
credited and that the original
publication in this journal is cited, in
accordance with accepted academic
practice. No use, distribution or
reproduction is permitted which does
not comply with these terms.

Formation of picosecond laser-induced periodic surface structures on steel for knee arthroplasty prosthetics

Zikrulloh Khuzhakulov¹, Salizhan Kylychbekov¹,
Yaran Allamyradov¹, Inomjon Majidov¹, Justice Ben Yosef²,
Alper Yusuf Er³, Chazz Kitchens⁴, Simran Banga⁴,
Sameer Badarudeen⁵ and Ali Oguz Er^{1*}

¹Department of Physics, Western Kentucky University, Bowling Green, KY, United States, ²Department of Chemistry, Western Kentucky University, Bowling Green, KY, United States, ³Bowling Green High School, Bowling Green, KY, United States, ⁴Department of Biology, Western Kentucky University, Bowling Green, KY, United States, ⁵The College of Medicine, University of Kentucky, Bowling Green, KY, United States

The formation of laser-induced periodic surface structures (LIPSS) on mirror-polished 304-grade stainless steel sheets with dimensions 25 mm × 25 mm × 0.8 mm upon irradiation with picosecond laser pulses in air and water environments at different wavelengths, number of pulses, and laser energy densities was investigated. Atomic force microscopy (AFM) and scanning electron microscopy (SEM) were used to characterize the LIPSS. Tunable periodicity of the LIPSS was observed in both media at different wavelengths and fluence. Fluence was shown to be the main formation parameter of LIPSS; however, the medium was also demonstrated to play an important role. Our results show that LIPSS can be successfully generated on stainless steel in a single-step process and that they can be easily modified by adjusting laser parameters.

KEYWORDS

LIPSS, picosecond laser, knee arthroplasty, stainless steel, surface morphology

Introduction

Laser-induced periodic surface structures (LIPSS) are a phenomenon that occurs due to intensive irradiation of surface material by linearly polarized light near the ablation threshold. LIPSS have been studied extensively on a variety of metals, semiconductors, and dielectrics (Gräf and Müller, 2015; Kru"ger and Kautek, 1996; Bonse et al., 2017; Bonse et al., 2012). LIPSS offer a fast, environmentally friendly, and cost effective manufacturing process for use in optics, medicine, tribology, and energy technologies.

Arrays of linear structures with sizes comparable to laser wavelength are observed. The shape and orientation of the surface morphology depend mainly on the polarization of the incoming light as well as the fluency, wavelength, pulse width, incidence angle, and other properties inherent to the experimental environment, such as the refractive index

and thermal conductivity of the media (Shukla et al., 2016; Kobayashi et al., 2019; Rivera et al., 2021; Zhang et al., 2021). Modifications in liquid (water) were shown to be more intensive than in a gaseous (air) medium when a titanium surface was modified by picosecond laser pulses (Trtica et al., 2018). A titanium surface with LIPSS exhibited a twofold decrease in surface friction as compared to untreated titanium (Bonse et al., 2017). Moreover, a laser-structured surface on a zirconia dental implant presented improved wetting, thermal load resistance, osseointegration, and less contamination (Delgado-Ruiz et al., 2011).

Although the formation and nature of the LIPSS are not completely understood, proposed explanations are divided into electromagnetic theories describing the transfer of optical energy into the material and the matter reorganization theory based on homogenous irradiation, solidification, and surface acoustic waves (Bonse and Gräf, 2020). It is widely thought that electromagnetic scattering and interference are responsible for the observed surface structures in addition to the excitation of surface plasmon polaritons (SPP) (Bonse et al., 2016; Bonse and Gräf, 2021).

LIPSS are divided into low spatial frequency (LSFL) and high spatial frequency (HSFL) structures based on their spatial periodicity, Λ . While the interference model can be applied to describe the mechanism of LSFL, it fails to describe HSFL due to its smaller periodicity than the laser wavelength. Self-organization, second harmonic generation, and surface plasmon excitation models were proposed for HSFL (Sipe et al., 1983; Albu et al., 2013). However, none of these models adequately explain the formation of LIPSS.

The surface functionalization that can be achieved in a single-step process when creating LIPSS can change optical, mechanical, or chemical surface properties (Hauschwitz et al., 2021). For instance, control of the wetting properties of stainless steel was achieved using LIPSS created at different laser fluences (Indrišiūnas et al., 2022). In addition, it was shown that LIPSS could significantly improve the absorbance of the steel sample (Wang et al., 2020). The microholes in stainless steel trepanned in one step using a circularly polarized femtosecond laser with the generation of varied LIPSS on the internal surface were investigated. The direction of the LIPSS was mainly perpendicular to the absorbed field direction (Hu et al., 2016). A novel structure was discovered when femtosecond laser double-pulse trains were used to produce LIPSS on 304 stainless steel (Li et al., 2021). It was claimed that the observed structure was due to the weak energy coupling of subpulses when the intrapulse delay was longer than the thermal relaxation time of stainless steel.

It should be noted that while there have been some studies on steel-based LIPSS (Cunha et al., 2015; Shinonaga et al., 2015; Cunha et al., 2016; Gregorčič et al., 2016; Epperlein et al., 2017; Huang et al., 2022a; Huang et al., 2022b; Gong et al., 2022), our study is novel in terms of the pulse width and laser fluence regime used. Ultrashort

laser pulses, such as picosecond and femtosecond laser pulses, can drive materials into highly non-equilibrium transient states. When the laser pulses first interact with the surface, the shielding effect of plasma that is created on a material's surface, which reflects and scatters the incident beam, determines how well the laser vaporizes the material. Femtosecond lasers are known to be more effective than nanosecond and picosecond lasers because they do not interact with the plasma surface and terminate before the heat is dispersed on the surface. In our study, we specifically use a picosecond laser because its pulse width is on the same order as the energy relaxation time. Therefore, understating the mechanism of how a picosecond laser creates LIPSS is crucial. In this study, we investigated the effects of laser fluence, wavelength, number of pulses, and medium on the formation of LIPSS on steel and titanium. Our results show that both wavelength and fluence have a direct effect on the morphology of each sample.

Experimental setup

Two different lasers, a Helios (1064-5-50) and a Helios (532-3-50), were focused on the sample surface with a nearly normal incidence in air and water. The laser beam has a near Gaussian shape (TEM00). Both lasers have a maximum repetition rate of 50 kHz, with a 2.5 mm beam diameter for 1,064 nm and 2 mm for 532 nm. The beams were expanded by 2× telescoping lenses to 5 mm and 4 mm, respectively. A lens with a focal length of 50 mm was used to focus the beam on the sample, resulting in a focal spot of 16.9 μm for 1064 nm and 8.47 μm for 532 nm. The measured powers at a 50 kHz repetition rate immediately after the telescoping lenses were 4.1 W and 2.7 W for 1,064 nm and 532 nm, respectively. Both lasers emit a vertically polarized beam with a pulse duration of 690 ps. The polarization of the beam ablating the surface of the sample was horizontal.

The material used in all experiments was a sheet of #8 finish mirror-polished 304-grade stainless steel, which is a commonly used industrial material, with dimensions 25 mm \times 25 mm \times 0.8 mm. Its surface was ultrasonically cleaned in acetone for 5 min before each experiment. The height of the water above the target during ablation in a water medium was 4 mm. The target was placed inside an open-top polystyrene box with dimensions 65 mm \times 65 mm \times 12 mm. The box was placed on a 3D positioning system with three linear stages, each with a resolution of 0.8 μm . The z -direction was parallel to the beam path. Patterns were obtained for different ablation times, using an electronic shutter to accurately measure the time of ablation. In order to verify the modified surface morphology, a scanning electron microscope (Model: JEOL JSM-6510LV) in high vacuum SEI mode with a 20 kV beam energy and an atomic force microscope were used. The AFM system used was a PicoPlus2 with a PicoView 1.20.3 software interface, operated in tapping mode.

Results and discussion

Effect of fluence and number of pulses

We performed several experiments to understand the effects of laser parameters, especially the optimal laser fluence and number of pulses required to obtain high-quality LIPSS. Different LIPSS were obtained in air and water media with 1,064 and 532 nm ps laser pulses. Initially, the effects of laser fluence and number of pulses were studied. The average fluence for an unfocused beam in front of the lens is $4.3 \times 10^{-4} \text{ J/cm}^2$ for 532 nm and $4.2 \times 10^{-4} \text{ J/cm}^2$ for 1,064 nm. The laser fluence and number of pulses appear to be the parameters that most influence the morphology. It is known that laser fluence plays a critical role in laser-material interaction (Farha et al., 2012; Mahmood et al., 2009; Farha et al., 2012; Fornarini et al., 2006; Lippert et al., 1993). We previously found that laser fluence has a significant effect on thin film and nanoparticle properties, such as size, surface roughness, number of particles, and film density (Farha et al., 2012; Belevov et al., 2020; Kholikov et al., 2018; Hakimov et al., 2022).

The effect of fluence on the formation of LIPSS has been investigated and the periodicity was shown to depend on the fluence (Umm et al., 2016; Xu et al., 2018). A transition from HSFL to LSFL was observed when a critical fluence threshold was exceeded (Xu et al., 2018). The morphology and periodicity of the LIPSS were observed to change with laser fluence (Höhm et al., 2012; Yao et al., 2017).

The effect of fluence on tool steel was investigated using picosecond laser pulses at different polarizations (Gregorčič et al., 2016). The authors showed that when the sample is significantly out of focus (low fluence), only HSFL occurs, parallel to the polarization and lower than the incident wavelength. Figure 1 shows the LIPSS formed at different fluences, parallel to the polarization of the laser beam in a water medium.

The fluence was adjusted by changing the distance between the lens and the target. Our results clearly indicate that fluence directly affects the morphology and periodicity of the pattern. Initially, a grating-like structure was obtained. As the fluence approaches the focal point, i.e., $z \sim 7 \text{ mm}$, the initial grating-like structure becomes prominent, individual three-dimensional structures become bigger, and periodicity increases. Our results also show that even near the ablation point, picosecond laser pulses can still produce LIPSS inside the focal spot area, where melt spots are also observed. Once the fluence exceeds the ablation threshold, LIPSS are no longer observed, and the laser simply removes the materials. It is known that the number of pulses affects the morphology and periodicity (Miyagawa et al., 2020; Rivera et al., 2021). The effect of the number of pulses (1 s–8 s) on LIPSS was investigated, as shown in Figure 2. It can be seen that when the laser hits the target for one second (50 kHz), the LIPSS are clearly observable, and the periodicity is comparable to the wavelength. The periodicity is (a) $\sim 1500 \text{ nm}$, (b) $\sim 1800 \text{ nm}$, and (c) $\sim 2700 \text{ nm}$.

When the number of pulses is doubled, the periodic structure becomes more prominent, the morphology of the pattern changes,

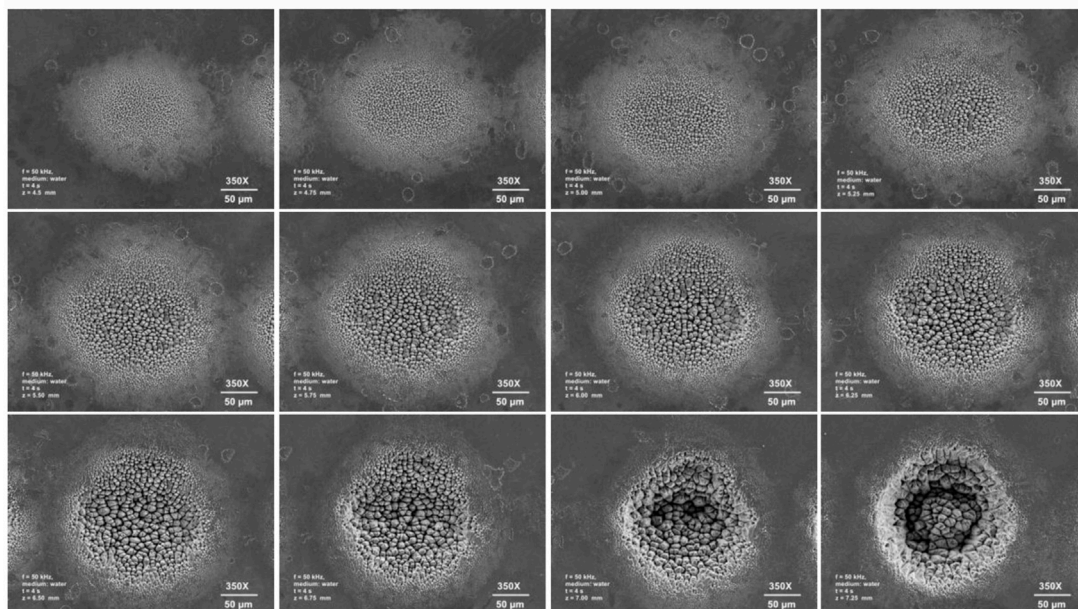


FIGURE 1
The effect of the fluence of 1,064 nm picosecond pulses in water on stainless steel LIPSS. The fluence was changed by moving the sample away from the focal point, thus increasing the area of irradiation and lowering the fluence.

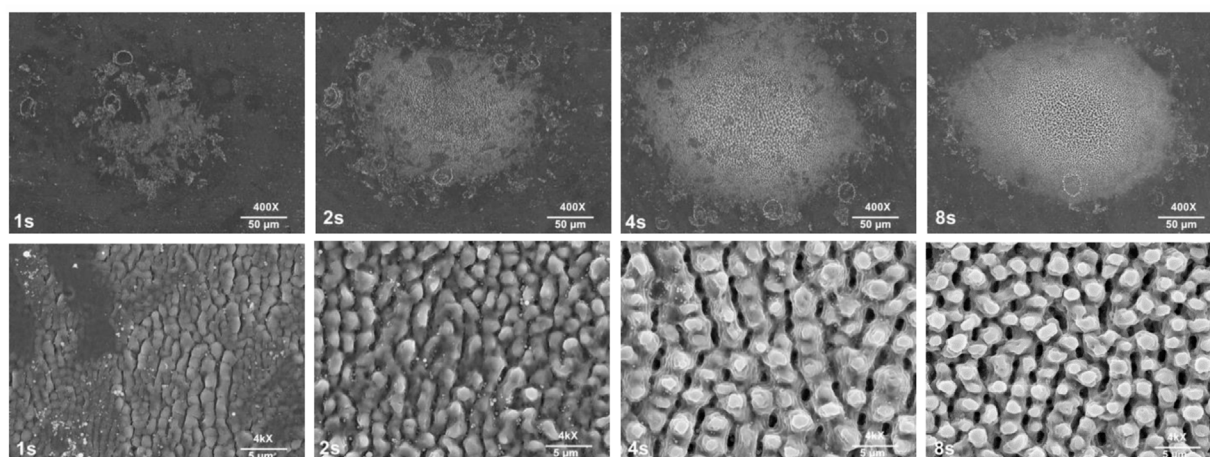


FIGURE 2

The effect of the number of 1,064 nm picosecond pulses in water at $z = 4.5$ mm on stainless steel LIPSS.

and the aspect ratio of the individual structure also changes. When the number of pulses is increased three times, the morphology changes again. More square-shaped structures are observed while the periodicity remains the same. A further increase in the number of pulses (4×50 kHz) caused a small change in morphology, and the periodicity remained relatively similar.

Effect of medium

The effect of medium (vacuum and O_2) on titanium LIPSS was investigated (Umm et al., 2016). It was shown that the periodicity of nano-scale LIPSS was higher in the case of irradiation under vacuum conditions as compared to under O_2 , and O_2 reduced the ablation threshold and revealed new phases (Umm et al., 2016). It is known that when a laser is absorbed in a confined medium, the peak pressure value increases up to 10-fold. This increase in pressure eventually changes the structures formed on the surface.

The laser absorption depth and the amount of material removed by a single laser pulse depend on the material's optical properties, the laser wavelength, and the laser energy density.

The properties of laser-produced plasma, such as the degree of ionization and the temperature of the plasma species, can evolve quickly and strongly and depend on many parameters such as the laser wavelength, energy density, repetition rate, pulse duration, spot size on target, target composition, and surface quality (Amoruso et al., 1999; Berthe et al., 1999). The laser pulse energy is initially predominantly absorbed by surface electrons leading to a sharp temperature gradient in the penetration depth and plasma formation. The material experiences a phase transformation from solid to vapor, and a pressure (shock)

wave is generated and propagates through the depth of the sample (Er et al., 2012). The energy is redistributed between the energy of the plume and the shock waves during expansion (Chrissey and Hubler, 1994; Eason, 2007). In laser-produced confined plasma, a transparent overlay is essential, where enhanced pressure (4–10 times higher) on the material surface must be achieved in order to produce a strong shock wave (Fabbro et al., 1990). Plastic deformations occur as the shock wave travels through the substrate. The confined plasma is essential when a sample is imprinted using laser shock wave propagation (Ilhom et al., 2018a; Ilhom et al., 2018b).

We also studied the effect of the medium on LIPSS. Samples were placed in air and water. Figure 1 shows the LIPSS on steel in a water medium at $z = 4.5$ mm. Figure 3 shows a similar measurement performed with the same fluence in air. It can be seen that LIPSS are barely observable in the air medium, whereas a clear pattern can be observed in water, even for 1 s irradiation. As the number of pulses increase in air, the LIPSS become more prominent, particularly after 4 s (periodicity ~ 850 nm) and 8 s (periodicity $\sim 1,000$ nm). Compared with the same condition in water, the LIPSS are formed in a more self-ordered manner in air, while structures formed in the water medium contain more grooves and hierarchical structures in the form of spikes and three-dimensional huts. Our results clearly show that the medium affects both the morphology and periodicity of the LIPSS.

Effect of wavelength on LIPSS

Both fluence and wavelength can change the electric field intensity distribution and the electron density, which are related to the periodicity and morphology of LIPSS (Wang et al., 2012;

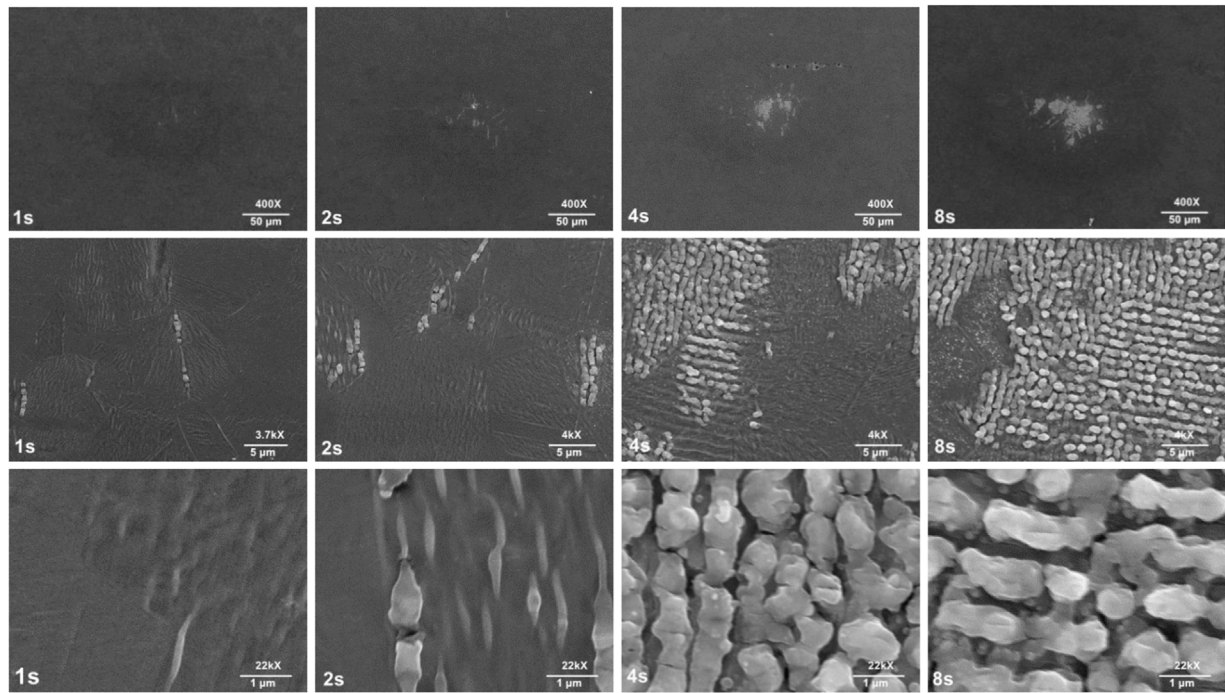


FIGURE 3
The effect of the fluence of 1,064 nm picosecond pulses in air at $z = 4.5$ mm on stainless steel LIPSS.

Lebugle et al., 2014; Kodama et al., 2020). The absorption process is directly dependent on the wavelength of the irradiation.

The LIPSS created by the 1064-nm laser wavelength were taller than those created by the 532-nm laser wavelength (Kodama et al., 2020). A significant difference between the damage threshold and the depth of the damage was seen when various wavelengths were used on the surface of an Inconel 600 superalloy (Staišić et al., 2012).

We investigated the effect of the wavelength on a steel surface in a water medium. Figure 4 clearly shows that, compared with the 1064-nm-wavelength laser, the 532-nm-wavelength laser

required less energy density to produce LIPSS because it is absorbed deeper into the substrate. In addition, the morphology differs significantly. While the morphology produced by the 532 nm laser is more akin to a circular structure, the 1,064 nm laser produced a more channel-type structure, with a distinct boundary.

Figure 4A shows an interesting result. Because the beam is Gaussian, the intensity is highest in the center of the beam. Therefore, a differential fluence is expected in the beam axis. In fact, this is manifested as differences in the pattern between the center and edge of the beam in some LIPSS patterns. For instance,

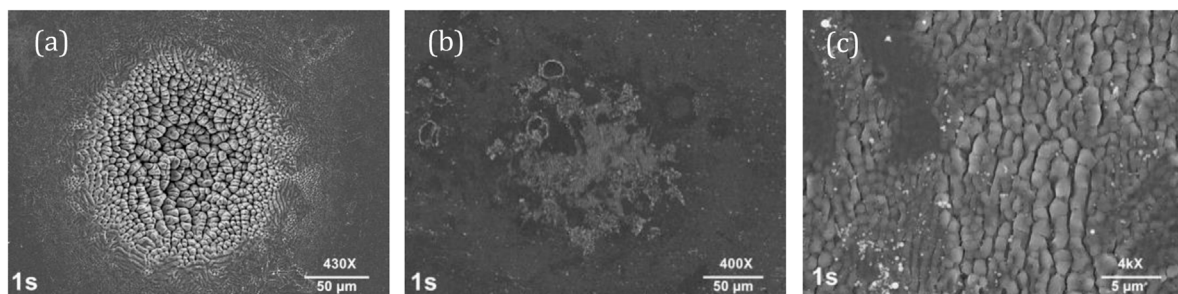


FIGURE 4
The effect of wavelength. (A) 532 nm and (B and C) 1,064 nm picosecond pulses in air at $z = 4.5$ mm in water.

Figure 4A shows a grating-like structure in the center and the onset of LSFL formation can be observed in the outer region of the beam; a channel-like structure with distinct periodicity begins to appear toward the edge of the beam.

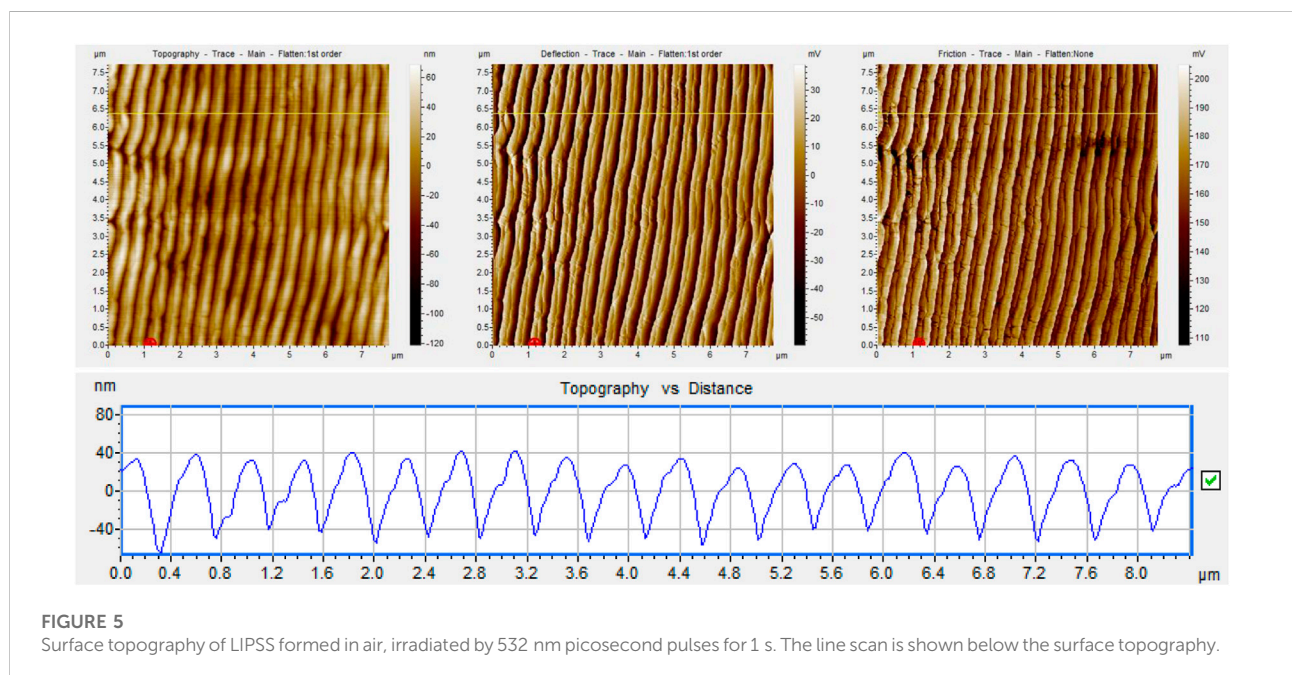
Figure 5 shows an AFM image of the LIPSS obtained in water using 532 nm ps laser pulses. The periodicity of the LIPSS is ~400 nm, which is comparable to the wavelength. It is clear that LSFL can be obtained under this condition.

Potential use of LIPSS on biofilm

Unlike conventional patterning methods, which are slow and expensive, laser patterning is inexpensive, environmentally friendly, very fast, with minimal distortion, and does not involve any heating or etching process (Ye and Cheng, 2012). LIPSS have been used to modify the optical, mechanical, and chemical properties of many materials (Florian et al., 2020). It has been shown that hierarchical spike structures produced by LIPSS on the surface of a Ti6Al4V titanium alloy could be used for miniaturized pacemakers, avoiding the unwanted growth of fibroblast cells on their surfaces (Heitz et al., 2017; Trtica et al., 2018; Wang et al., 2020; Li et al., 2021). Micro-patterned surfaces have also been shown to decrease the surface attachment of numerous microorganisms and to reduce biofilm formation *in vitro* (May et al., 2014). It is known that frictional action at the prosthetic interface causes stresses within tissues; these stresses may damage the tissues and affect their normal functions. In addition, a titanium surface with LIPSS presented a twofold decrease in surface friction compared with untreated titanium

(Bonse et al., 2017). As stated earlier, the laser-structured surface on a zirconia dental implant exhibited improved wetting, thermal load resistance, osseointegration, and less contamination (Delgado-Ruiz et al., 2011). In addition to the physical properties of the surface, the chemical composition of the surface can affect a range of cellular behaviors (Dykas et al., 2018). Stainless steel possesses a chromium oxide layer that forms when chromium reacts with oxygen. This reaction is instant, with formation speeds measured to be in the nanosecond range, and layer thicknesses up to the micron range. The presence of Al₂O₃ and NdGaO₃ reduced biofilms' effectiveness by approximately 20% and 40%, respectively, compared with the control (100%), while zinc oxide had the highest impact (Dykas et al., 2018). Stainless steel 316 is a chromium-nickel austenitic stainless steel with added molybdenum, which provides greater resistance to corrosion and pitting. However, it should be noted that although stainless steel possesses an oxide layer, various microorganisms have the ability to adhere to and produce biofilms on stainless steel surfaces (de Castro et al., 2017; AwadTarek et al., 2018; Dula and Ajayeoba, 2021). In fact, *E. coli* was shown to directly adhere to the passive surface instead of the metallic surface. Therefore, bacterial alteration and deterioration of this oxide layer is a significant problem for the reliability and integrity of steel structures (Seyeux et al., 2015).

Motivated by the benefits of LIPSS, our LIPSS will be further evaluated in terms of biofilm formation efficiency. This goal is extremely critical for prosthetic implants because surface roughness and texture can drastically alter the characteristics of drag and friction forces exerted on the surface of a moving object in a fluid (Jimenez, 2004; Thill et al., 2008).



Summary

The formation of LIPSS on mirror-polished 304-grade stainless steel by picosecond laser pulses in air and water environments at different laser wavelengths and densities was investigated. LIPSS were observed to have tunable periodicity in both mediums at different wavelengths and fluence. Fluence was shown to be the main formation parameter of LIPSS, while the medium, number of pulses, and wavelength also play important roles. Our results show that surface patterns can be easily modified by adjusting the main laser parameters. Overall, our work demonstrates that LIPSS are a powerful single-step tool for the fabrication of multiple patterns on a stainless steel surface. These results shed new light on the formation mechanism of LIPSS using a picosecond laser in water and air. In the future, biofilm formation on LIPSS will be evaluated as a preventive measure for prosthetic joint infection.

Data availability statement

The original contributions presented in the study are included in the article/Supplementary Material; further inquiries can be directed to the corresponding author.

Author contributions

All authors listed have made a substantial, direct, and intellectual contribution to the work and have approved it for publication.

References

- Albu, C, Adrian, D, Filipescu, M, Ulmeanu, M, and Zamfirescu, M (2013). Periodical structures induced by femtosecond laser on metals in air and liquid environments. *Appl. Surf. Sci.* 278, 347–351. doi:10.1016/j.apsusc.2012.11.075
- Amoruso, S, Bruzzese, R, Spinelli, N, and Velotta, R. (1999). Characterization of laser-ablation plasmas. *J. Phys. B At. Mol. Opt. Phys.* 32, 131–172. doi:10.1088/0953-4075/32/14/201
- AwadTarek, S., Asker, D., and Hatton, B. D. (2018). Food-safe modification of stainless steel food-processing surfaces to reduce bacterial biofilms. *ACS Appl. Mat. Interfaces* 10 (27), 22902–22912. doi:10.1021/acsami.8b03788
- Belekov, E, Kholikov, K, Cooper, L, Banga, S, and Er, A O. (2020). Improved antimicrobial properties of methylene blue attached to silver nanoparticles. *Photodiagnosis Photodyn. Ther.* 32, 102012. doi:10.1016/j.pdpdt.2020.102012
- Berthe, L., Fabbro, R., Peyre, P., and Bartnicki, E. (1999). Wavelength dependent of laser shock-wave generation in the water-confinement regime. *J. Appl. Phys.* 85, 7552–7555. doi:10.1063/1.370553
- Bonse, J., Höhm, S., Kirner, S. V., Rosenfeld, A., and Krüger, J. (2017). Laser-induced periodic surface structures—a scientific evergreen. *IEEE J. Sel. Top. Quantum Electron.* 23 (3). doi:10.1109/JSTQE.2016.2614183
- Bonse, J., Krüger, J., Höhm, S., and Rosenfeld, A. (2012). Femtosecond laser-induced periodic surface structures. *J. Laser Appl.* 24 (4), 042006. doi:10.2351/1.4712658
- Bonse, J, and Gräf, S (2020). Maxwell meets marangoni—a review of theories on laser-induced periodic surface structures. *Laser & Photonics Rev.* 14 (10), 2000215. doi:10.1002/lpor.202000215
- Bonse, J, and Gräf, S (2021). Ten open questions about laser-induced periodic surface structures. *Nanomaterials* 11, 3326. doi:10.3390/nano11123326

Funding

This project is supported by the Kentucky Biomedical Research Infrastructure Network and INBRE (KBRIN) ULRF13-1493C-01, NSF KY EPSCoR RA (3200002692-23-011), and NSF MRI (Award Number: 1920069).

Acknowledgments

We would like to thank Dr John Andersland for SEM measurements.

Conflict of interest

The authors declare that the research was conducted in the absence of any commercial or financial relationships that could be construed as a potential conflict of interest.

Publisher's note

All claims expressed in this article are solely those of the authors and do not necessarily represent those of their affiliated organizations, or those of the publisher, the editors, and the reviewers. Any product that may be evaluated in this article, or claim that may be made by its manufacturer, are not guaranteed or endorsed by the publisher.

Bonse, J, Höhm, S, Kirner, S, Rosenfeld, A, and Krüger, J (2016). “Laser-induced periodic surface structures (LIPSS) – a scientific evergreen,” in Conference on Lasers and Electro-Optics (California, CA, USA: Optica Publishing Group).

Chrisey, D. B., and Hubler, G. K. (1994). *Pulsed laser deposition of thin films*. New York, NY, USA: Wiley Inc.

Cunha, A, Anne-Marie, E, Laurent, P., Paula, S. A., Maria, B. dR. A., Amélia, A, et al. (2016). Femtosecond laser surface texturing of titanium as a method to reduce the adhesion of *Staphylococcus aureus* and biofilm formation. *Appl. Surf. Sci.* 360, 485–493. doi:10.1016/j.apsusc.2015.10.102

Cunha, A., Zouani, O. F., Plawinski, L., Botelho do Rego, A. M., Almeida, A., Vilar, R., et al. (2015). Human mesenchymal stem cell behavior on femtosecond laser-textured Ti-6Al-4V surfaces. *Nanomedicine* 10, 725–739. doi:10.2217/nnm.15.19

Dula, S, and Ajayeoba, T. A. (2021). Bacterial biofilm formation on stainless steel in the food processing environment and its health implications. *Folia Microbiol. (Praha)*. 66 (3), 293–302. doi:10.1007/s12223-021-00864-2

de Castro, R, MarcíliaFernandes, M d S, Yorika, D, and Kuaye, Y (2017). Biofilm formation on stainless steel as a function of time and temperature and control through sanitizers. *Int. Dairy J.* 68, 9–16. doi:10.1016/j.idairyj.2016.12.005

Delgado-Ruiz, R. A., Calvo-Guirado, J. L., Moreno, P., Guardia, J., Gomez-Moreno, G., Mate-Sánchez, J. E., et al. (2011). Femtosecond laser microstructuring of zirconia dental implants. *J. Biomed. Mat. Res.* 96B (1), 91–100. doi:10.1002/jbm.b.31743

Dykas, M M., Desai, S K., Patra, A, Motapothula, M R, Poddar, K, Kenney, L J, et al. (2018). Identification of biofilm inhibitors by screening combinatorial libraries

- of metal oxide thin films. *ACS Appl. Mat. Interfaces* 10 (15), 12510–12517. doi:10.1021/acsami.8b02246
- Eason, R. (2007). *Pulsed laser deposition of thin films: Applications*. Hoboken, NJ, USA: John Wiley & Sons.
- Epperlein, N, Menzel, F, Schwibbert, K, Koter, R, Bonse, J, Sameith, J, et al. (2017). Influence of femtosecond laser produced nanostructures on biofilm growth on steel. *Appl. Surf. Sci.* 418, 420–424. doi:10.1016/j.apsusc.2017.02.174
- Er, A. O., Chen, J, Tang, J, and Rentzepis, P M. (2012). Coherent acoustic wave oscillations and melting on Ag(111) surface by time resolved x-ray diffraction. *Appl. Phys. Lett.* 100, 151910–151915. doi:10.1063/1.3703122
- Fabbro, R., Fournier, J., Ballard, P., Devaux, D., and Virmont, J. (1990). Physical study of laser-produced plasma in confined geometry. *J. Appl. Phys.* 68, 775–784. doi:10.1063/1.346783
- Farha, A. H., Er, A. O., Ufuktepe, Y., and Elsayed-Ali, H. E. (2012). Laser-fluence effects on NbNx thin films fabricated by pulsed laser deposition. *Mat. Chem. Phys.* 132, 667–672. doi:10.1016/j.matchemphys.2011.11.084
- Florian, C, Sabrina, V., Kruger, J., and Bonse, J. (2020). Surface functionalization by laser-induced periodic surface structures. *J. Laser Appl.* 32 (2), 022063. doi:10.2351/7.0000103
- Fornarini, L., Spizzichino, V., Colao, F., Fantoni, R., and Lazić, V. (2006). Influence of laser wavelength on LIBS diagnostics applied to the analysis of ancient bronzes. *Anal. Bioanal. Chem.* 385 (2), 272–280. doi:10.1007/s00216-006-0300-1
- Gong, N, Maharjan, N, Liu, H, Li, H, Feng, W, Luai, T, et al. (2022). Laser-induced in-plane curving of ripples on biomedical stainless steel and their relationship to biological functions. *Mater. Technol.* 37, 3089–3099. doi:10.1080/10667857.2022.2124074
- Gräf, S, and Müller, F A. (2015). Polarisation-dependent generation of fs-laser induced periodic surface structures. *Appl. Surf. Sci.* 331, 150–155. doi:10.1016/j.apsusc.2015.01.056
- Gregoričič, P, Sedlaček, M, Podgornik, B, and Reif, J (2016). Formation of laser-induced periodic surface structures (LIPSS) on tool steel by multiple picosecond laser pulses of different polarizations. *Appl. Surf. Sci.* 387, 698–706. doi:10.1016/j.apsusc.2016.06.174
- Hakimov, S, Kylychbekov, S, Harness, B, Neupane, S, Hurley, J, Brooks, A, et al. (2022). Evaluation of silver nanoparticles attached to methylene blue as an antimicrobial agent and its cytotoxicity. *Photodiagnosis Photodyn. Ther.* 39, 102904. doi:10.1016/j.pdpdt.2022.102904
- Hauschwitz, P., Martan, J., Bičičková, R., Beltrami, C., Moskal, D., Brodsky, A., et al. (2021). LIPSS-based functional surfaces produced by multi-beam nanostructuring with 2601 beams and real-time thermal processes measurement. *Sci. Rep.* 11 (1), 22944. doi:10.1038/s41598-021-02290-3
- Heitz, J., Plamadéala, C., Muck, M., Armbruster, O., Baumgartner, W., Weth, A., et al. (2017). Femtosecond laser-induced microstructures on Ti substrates for reduced cell adhesion. *Appl. Phys. A* 123 (12), 734. doi:10.1007/s00339-017-1352-0
- Höhm, S., Rosenfeld, A., Krüger, J., and Bonse, J. (2012). Femtosecond laser-induced periodic surface structures on silica. *J. Appl. Phys.* 112 (1), 014901. doi:10.1063/1.4730902
- Hu, Y, Fan, N, Lu, Y, Sun, X, Wang, C, Xia, Z, et al. (2016). LIPSS formed on the sidewalls of microholes in stainless steel trepanned by a circularly polarized femtosecond laser. *Appl. Phys. A* 122 (7), 665. doi:10.1007/s00339-016-0167-8
- Huang, J, Liu, Y, Jin, S, Wang, Z, Qi, Y, Zhang, J, et al. (2022). Uniformity control of laser-induced periodic surface structures. *Front. Phys.* 10. doi:10.3389/fphy.2022.932284
- Huang, J, Xu, K, Xu, S, Li, X, and Wei, Q-H (2022). Self-aligned laser-induced periodic surface structures for large-area controllable nanopatterning. *Laser & Photonics Rev.* 16 (8), 2200093. doi:10.1002/lpor.202200093
- Ihrom, S., Kholikov, K., Ottman, C., Sanford, D., Thomas, Z., San, O., et al. (2018). Scalable patterning using laser-induced shock waves. *Opt. Eng.* 57, 1–6. doi:10.1117/1.oe.57.4.041413
- Ihrom, S., Seyitliyev, D., Kholikov, K., Thomas, Z., Li, P., Karaca, H. E., et al. (2018). Laser shock wave-assisted patterning on NiTi shape memory alloy surfaces. *Shap. Mem. Superelasticity* 4, 224–231. doi:10.1007/s40830-018-0146-3
- Indrišūnas, S, Svirplys, E, and Gedvilas, M (2022). Large-area fabrication of LIPSS for wetting control using multi-parallel femtosecond laser processing. *Materials* 15 (16), 5534. doi:10.3390/ma15165534
- Jimenez, J. (2004). Turbulent flows over rough walls. *Annu. Rev. Fluid Mech.* 36, 173–196. doi:10.1146/annurev.fluid.36.050802.122103
- Kholikov, K., Ihrom, S., Sajjad, M., Smith, M. E., Monroe, J. D., San, O., et al. (2018). Improved singlet oxygen generation and antimicrobial activity of sulphur-doped graphene quantum dots coupled with methylene blue for photodynamic therapy applications. *Photodiagnosis Photodyn. Ther.* 24, 7–14. doi:10.1016/j.pdpdt.2018.08.011
- Kobayashi, T, Wakabayashi, T, Takushima, Y, and Yan, J (2019). Formation behavior of laser-induced periodic surface structures on stainless tool steel in various media. *Precis. Eng.* 57, 244–252. doi:10.1016/j.precisioneng.2019.04.012
- Kodama, S, Shimada, K, Mizutani, M, and Kuriyagawa, T (2020). Effects of pulse duration and heat on laser-induced periodic surface structures. *Int. J. Automation Technol.* 14 (4), 552–559. doi:10.20965/ijat.2020.p0552
- Kruger, J., and Kautek, W. (1996). Femtosecond-pulse visible laser processing of transparent materials. *Appl. Surf. Sci.* 96, 430–438. doi:10.1016/0169-4332(95)00446-7
- Lebugle, M., Sanner, N., Uteza, O., and Sents, M. (2014). Guidelines for efficient direct ablation of dielectrics with single femtosecond pulses. *Appl. Phys. A* 114, 129–142. doi:10.1007/s00339-013-8153-x
- Li, Y, Hu, J, Liu, W, Yin, J, and Lu, J (2021). High period frequency LIPSS emerging on 304 stainless steel under the irradiation of femtosecond laser double-pulse trains. *Chin. Opt. Lett.* 19 (12), 123801. doi:10.3788/col202119.123801
- Lippert, T., Stebani, J., Ihlemann, J., Nuyken, O., and Wokaun, A. (1993). Excimer laser ablation of novel triazine polymers: Influence of structural parameters on the ablation characteristics. *J. Phys. Chem.* 97 (47), 12296–12301. doi:10.1021/j100149a033
- Mahmood, S., Rawat, R. S., Zakaullah, M., Lin, J. J., Springham, S. V., Tan, T. L., et al. (2009). Investigation of plume expansion dynamics and estimation of ablation parameters of laser ablated Fe plasma. *J. Phys. D: Appl. Phys.* 42 (13), 135504. doi:10.1088/0022-3727/42/13/135504
- May, R M., Hoffman, M G., Sogo, M J., Parker, A E., O'Toole, G A., Brennan, A B., et al. (2014). Micro-patterned surfaces reduce bacterial colonization and biofilm formation *in vitro*: Potential for enhancing endotracheal tube designs. *Clin. Transl. Med.* 3 (1), 8. doi:10.1186/2001-1326-3-8
- Miyagawa, R., Ohgai, T., and Eryu, O. (2020). “Effect of pulse interval and pulse numbers on the formation of laser-induced periodic nanostructures,” in *Laser congress 2020 (ASSL, LAC)*. OSA technical digest. Editors P. Schunemann, C. Saraceno, S. Mirov, S. Taccheo, J. Nilsson, A. Petersen, et al. (Washington, DC: Optica Publishing Group).
- Rivera, L. P., Munoz-Martín, D., Chávez-Chávez, A., Morales, Miguel, Gómez-Rosas, G., and Molpeceres, C. (2021). Subwavelength LIPSS formation on SS304 by picosecond laser irradiation under water confinement. *Mater. Sci. Eng. B* 273, 115393. doi:10.1016/j.mseb.2021.115393
- Seyeux, A, Zanna, S, Allion, A, and Marcus, P (2015). The fate of the protective oxide film on stainless steel upon early stage growth of a biofilm. *Corros. Sci.* 91, 352–356. doi:10.1016/j.corsci.2014.10.051
- Shinonaga, T., Tsukamoto, M., Kawa, T., Chen, P., Nagai, A., and Hanawa, T. (2015). Formation of periodic nanostructures using a femtosecond laser to control cell spreading on titanium. *Appl. Phys. B* 119, 493–496. doi:10.1007/s00340-015-6082-4
- Shukla, P., Waugh, D. G., Lawrence, J., and Vilar, R. (2016). “Laser surface structuring of ceramics, metals and polymers for biomedical applications: A review,” in *Laser surface modification of biomaterials*. Editor R. Vilar (Cambridge, UK: Woodhead Publishing), 281–299.
- Sipe, J. E., Young, J F., Preston, J. S., and van Driel, H. M. (1983). Laser-induced periodic surface structure. I. Theory. *Phys. Rev. B* 27 (2), 1141–1154. doi:10.1103/physrevb.27.1141
- Stajić, J., Gaković, B., Trtica, M., Desai, T., and Volpe, L. (2012). Superficial changes on the Inconel 600 superalloy by picosecond Nd:YAG laser operating at 1064, 532, and 266 nm: Comparative study. *Laser Part. Beams* 30 (2), 249–257. doi:10.1017/s0263034611000899
- Thill, C., Etches, J., Bond, I., Potter, K., and Weaver, P. (2008). Morphing skins. *Aeronaut. J.* 112, 117–139. doi:10.1017/s000192400002062
- Trtica, M., Stasic, J., Batani, D., Benocci, R., Narayanan, V., and Ciganovic, J. (2018). Laser-assisted surface modification of Ti-implant in air and water environment. *Appl. Surf. Sci.* 428, 669–675. doi:10.1016/j.apsusc.2017.09.185
- Umm, i., Kalsoom Bashir, S, Ali, N, Shahid Rafique, M., Husinsky, W, et al. (2016). Effect of fluence and ambient environment on the surface and structural modification of femtosecond laser irradiated Ti*. *Chin. Phys. B* 25 (1), 018101. doi:10.1088/1674-1056/25/1/018101
- Wang, C., Jiang, L., Wang, F., Li, X., Yuan, Y., Xiao, H., et al. (2012). First-principles electron dynamics control simulation of diamond under femtosecond

laser pulse train irradiation. *J. Phys. Condens. Matter* 24, 275801. doi:10.1088/0953-8984/24/27/275801

Wang, T, Bian, J, Li, X, Kong, H, Wang, L, Wang, X, et al. (2020). Enhanced absorbance of 45# steel by laser-induced periodic surface structures (LIPSS). *Metals* 10 (9), 1237. doi:10.3390/met10091237

Xu, S-z, Dou, H-q, Sun, K, Ye, Y-y, Li, Z, Wang, H-j, et al. (2018). Scan speed and fluence effects in femtosecond laser induced micro/nano-structures on the surface of fused silica. *J. Non. Cryst. Solids* 492, 56–62. doi:10.1016/j.jnoncrysol.2018.04.018

Yao, C, Ye, Y, Jia, B, Yuan, L, Ding, R, Jiang, Y, et al. (2017). Polarization and fluence effects in femtosecond laser induced micro/nano structures on stainless steel with antireflection property. *Appl. Surf. Sci.* 425, 1118–1124. doi:10.1016/j.apsusc.2017.07.157

Ye, C., and Cheng, G. Y. (2012). Scalable patterning on shape memory alloy by laser shock assisted direct imprinting. *Appl. Surf. Sci.* 258, 10042–10046. doi:10.1016/j.apsusc.2012.06.070

Zhang, D, Liu, R, and Li, Z (2021). Irregular LIPSS produced on metals by single linearly polarized femtosecond laser. *Int. J. Extrem. Manuf.* 4 (1), 015102. doi:10.1088/2631-7990/ac376c